Online Appendix

"The Impact of Pessimistic Expectations on the Effects of COVID-19-Induced Uncertainty in the euro Area" by Giovanni Pellegrino, Federico Ravenna and Gabriel Züllig

Computation of the Generalized Impulse Response Functions

This Section documents the algorithm employed to compute the state-dependent GIRFs and their confidence intervals. The algorithm follows Koop, Pesaran, and Potter (1996), with the modification of considering an orthogonal structural shock, as in Kilian and Vigfusson (2011). The algorithm is the same used in Pellegrino (2017).

The theoretical GIRF of the vector of endogenous variables $\mathbf{Y}$, h periods ahead, for a starting condition $\boldsymbol{\varpi}_{t-1} = \{\mathbf{Y}_{t-1}, ..., \mathbf{Y}_{t-L}\}$, and a structural shock in date t, δ_t, can be expressed – following Koop, Pesaran, and Potter (1996) – as:

$$GIRF_{\mathbf{Y},t}(h, \delta_t, \boldsymbol{\varpi}_{t-1}) = \mathbb{E}\left[\mathbf{Y}_{t+h} \mid \delta_t, \boldsymbol{\varpi}_{t-1}\right] - \mathbb{E}\left[\mathbf{Y}_{t+h} \mid \boldsymbol{\varpi}_{t-1}\right], \quad h = 0, 1, \ldots, H$$

where $\mathbb{E}[\cdot]$ represents the expectation operator. We are interested in the state-dependent GIRFs for pessimistic and normal times, which can be defined as:

$$GIRF_{\mathbf{Y},t}\left(h, \delta_t, \boldsymbol{\Omega}_{t-1}^{pessimistic\ times}\right) = \mathbb{E}\left[GIRF_{\mathbf{Y},t}\left(h, \delta_t, \left\{\boldsymbol{\varpi}_{t-1} \in \boldsymbol{\Omega}_{t-1}^{pessimistic\ times}\right\}\right)\right]$$

$$GIRF_{\mathbf{Y},t}\left(h, \delta_t, \boldsymbol{\Omega}_{t-1}^{normal\ times}\right) = \mathbb{E}\left[GIRF_{\mathbf{Y},t}\left(h, \delta_t, \left\{\boldsymbol{\varpi}_{t-1} \in \boldsymbol{\Omega}_{t-1}^{normal\ times}\right\}\right)\right]$$

where $\boldsymbol{\Omega}_{t-1}^{i}$ denotes the set of histories characterizing the state $i = \{pessimistic\ times, \quad normal\ times\}$.

The algorithm to estimate our state-conditional GIRF reads as follows:

1. pick an initial condition $\boldsymbol{\varpi}_{t-1} = \{\mathbf{Y}_{t-1}, ..., \mathbf{Y}_{t-L}\}$, i.e., the historical values for the lagged endogenous variables at a particular date $t = L + 1, \ldots, T$. Notice that this set includes the values for the interaction terms;

2. draw randomly (with repetition) a sequence of (n-dimensional) residuals $\{\mathbf{u}_{t+h}\}^s$, $h = 0, 1, ..H = 19$, from the empirical distribution $d(\mathbf{0}, \widehat{\boldsymbol{\Omega}})$, where $\widehat{\boldsymbol{\Omega}}$ is the estimated VCV matrix. In order to preserve the contemporaneous structural relationships among variables, residuals are assumed to be jointly distributed, so that if date t' s residual is drawn, all n residuals for date

t are collected;

3. conditional on $\boldsymbol{\varpi}_{t-1}$ and on the estimated model (1), use the sequence of residuals $\{\mathbf{u}_{t+h}\}^s$ to simulate the evolution of the vector of endogenous variables over the following H periods to obtain the path $\mathbf{Y}^s_{t+h}$ for $h = 0, 1 \dots H$. s denotes the dependence of the path on the particular sequence of residuals used;

4. conditional on $\boldsymbol{\varpi}_{t-1}$ and on the estimated model (1), use the sequence of residuals $\{\mathbf{u}_{t+h}\}^s$ to simulate the evolution of the vector of endogenous variables over the following H periods when a structural shock δ_t is imposed to $\mathbf{u}^s_t$. In particular, we Cholesky-decompose $\widehat{\boldsymbol{\Omega}} = \mathbf{C}\mathbf{C}'$, where $\mathbf{C}$ is a lower-triangular matrix. Then, we recover the structural innovation associated with $\mathbf{u}^s_t$ by $\boldsymbol{\varepsilon}^s_t = \mathbf{C}^{-1}\mathbf{u}^s_t$ and add a quantity $\delta < 0$ to the scalar element of $\boldsymbol{\varepsilon}^s_t$ that refers to the uncertainty measure, i.e. $\varepsilon^s_{t,unc}$. We then move again to the residual associated with the structural shock $\mathbf{u}^{s,\delta}_t = \mathbf{C}\boldsymbol{\varepsilon}^{s,\delta}_t$ to proceed with simulations as in point 3. Call the resulting path $\mathbf{Y}^{s,\delta}_{t+h}$;

5. compute the difference between the previous two paths for each horizon and for each variable, i.e. $\mathbf{Y}^{s,\delta}_{t+h} - \mathbf{Y}^s_{t+h}$ for $h = 0, 1 \dots, H$;

6. repeat steps 2-5 for a number of $S = 500$ different extractions for the residuals and then take the average across s. Notice that in this computation the starting month $t-1$ does not change. In this way we obtain a consistent point estimate of the GIRF for each given starting month in our sample , i.e. $\widehat{GIRF}_{\mathbf{Y},t}(\delta_t, \boldsymbol{\varpi}_{t-1}) = \left\{\widehat{\mathbb{E}}\left[\mathbf{Y}_{t+h} \mid \delta_t, \boldsymbol{\varpi}_{t-1}\right] - \widehat{\mathbb{E}}\left[\mathbf{Y}_{t+h} \mid \boldsymbol{\varpi}_{t-1}\right]\right\}_{h=0}^{19}$. If a given initial condition $\boldsymbol{\varpi}_{t-1}$ brings an explosive response (namely if this is explosive for most of the sequences of residuals drawn $\{\mathbf{u}_{t+h}\}^s$, in the sense that the response of the variable shocked diverges instead of reverting to zero), it is discarded and not considered for the computation of state-conditional responses at the next step;[1]

7. repeat steps 2-6 to obtain an history-conditional GIRF for each initial condition $\boldsymbol{\varpi}_{t-1}$ of interest. In particular, we select two particular subsets of initial conditions related to the historical level of consumer confidence to define two states. An initial condition $\boldsymbol{\varpi}_{t-1} =$

[1] While we allow this to happen for bootstrapped simulated responses, we make sure that this does not happen for point-estimated responses (i.e. our responses estimated on actual data) so that to back up the stability of the estimated IVAR . The nonlinear DSGE literature has developed the pruning method in order to preserve stability (see Andreasen, Fernández-Villaverde, and Rubio-Ramírez (2017)) but this is not currently available for nonlinear VARs.

$\{\mathbf{Y}_{t-1}, ..., \mathbf{Y}_{t-L}\}$ is classified to belong to the "pessimistic times" state if $conf_{t-1}$ is in the bottom 20% of the consumer confidence empirical distribution and to the "normal times" state if $conf_{t-1}$ is in not in its bottom 20%;

8. history-dependent GIRFs obtained in step 7 are then averaged over the state they belong to produce our estimate of the state-dependent GIRFs, i.e., our $\widehat{GIRF}_{\mathbf{Y},t}\left(\delta_t, \mathbf{\Omega}_{t-1}^{pessimistic\ \ times}\right)$ and $\widehat{GIRF}_{\mathbf{Y},t}\left(\delta_t, \mathbf{\Omega}_{t-1}^{normal\ times}\right)$;

9. confidence bands around the point estimates obtained in point 8 are computed through bootstrap[2]. In particular, we simulate $R = 500$ datasets statistically equivalent to the actual sample and for each of them interaction terms are constructed coherently with the simulated series. Then, for each dataset, (i) we estimate our Interacted VAR model and (ii) implement steps 1-8. In implementing the procedure the starting conditions and the VCV matrix used in the computation depend on the particular dataset r used, i.e. $\boldsymbol{\varpi}_{t-1}^r$ and $\widehat{\mathbf{\Omega}}^r$. Of the resulting distribution of state-conditional GIRFs, we take the 5th and 95th percentiles to construct the 90% confidence bands.

Computation of the Generalized Forecast Error Variance Decomposition

The algorithm for the computation of the state-dependent Generalized Forecast Error Variance Decomposition (GFEVD) for our nonlinear VAR model follows Caggiano, Castelnuovo, and Pellegrino (2017). In particular, the innovations to the algorithm proposed in Lanne and Nyberg (2016) are: i) it is designed to simulate the importance of an orthogonal structural shock, and ii) it considers a one standard deviation shock in each variable. The expression at the basis of our computation of the GFEVD is the same proposed by Lanne and Nyberg (2016, equation 9).

In particular, conditional on a specific initial history $\boldsymbol{\varpi}_{t-1}$ and a forecast horizon of interest z, the $GFEVD_{ij}$ that refers to a variable i and a shock j whose size is δ_t^j is given by:

$$GFEVD_{ij}(z, \boldsymbol{\varpi}_{t-1}) = \frac{\sum_{h=0}^{z} GIRF_{Y_i}(h, \delta_t^j, \boldsymbol{\varpi}_{t-1})^2}{\sum_{j=1}^{n}\sum_{h=0}^{z} GIRF_{Y_i}(h, \delta_t^j, \boldsymbol{\varpi}_{t-1})^2} \qquad i, j = 1, ..., n, \tag{A1}$$

[2]The bootstrap used is similar to the one used by Christiano, Eichenbaum and Evans (1999, footnote 23). Our code repeats the explosive artificial draws to be sure that exactly 500 draws are used.

where h is an indicator keeping track of the forecast ahead, and n denotes the number of variables in the vector $\mathbf{Y}$.[3] Differently from Lanne and Nyberg (2016), in our case the object $GIRF_{Y_i}(\cdot)$ in the formula refers to GIRFs à la Koop, Pesaran, and Potter (1996) computed by considering an orthogonal shock as in Kilian and Vigfusson (2011).[4] In our application we are interested in the contribution of an identified uncertainty shock to the GFEVD of all the variables in the vector $\mathbf{Y}$. Further, while formula (A1) defines the GFEVD for a given history, we are interested in computing a state-conditional GFEVD referring to a set of histories.

Given our model (1), we compute our state-dependent GFEVD for normal times and pessimistic times by following the steps indicated below. In particular, we:

1. consider an orthogonal shock equal to a standard deviation in each variable of the estimated I-VAR model. This is equivalent, for a Cholesky decomposition, to taking a vector of shocks equal to $\left(\delta_t^1, \delta_t^2, ..., \delta_t^n\right) = (1, 1, ..., 1)$ in our algorithm in the previous Section;[5]

2. pick a history $\boldsymbol{\varpi}_{t-1}$ from the set of all histories;

3. compute the $GIRF_{\mathbf{Y}}(\cdot, \cdot, \boldsymbol{\varpi}_{t-1})$ for each δ_t^j $(j = 1, ..., n)$ and for each $h \leq z$ according to points 2-6 of the algorithm in the previous Section;

4. plug the GIRFs computed in step 3 into equation (A1) to obtain $GFEVD_{ij}(z, \boldsymbol{\varpi}_{t-1})$ for the particular forecast horizon z and history $\boldsymbol{\varpi}_{t-1}$ considered;

5. repeat steps 2–4 for all the histories, distinguishing between the histories belonging to the "normal times" state and the "pessimistic times" state (see the definition in point 7 of the GIRFs algorithm);

6. compute the state-dependent GFEVD for the "normal times" state and the "pessimistic times" state by computing the average of the $GFEVD_{ij}(z, \boldsymbol{\varpi}_{t-1})$ across all the histories relevant for the two states.

[3] Expression (A1) gives a GFEVD that by construction lies between 0 and 1, and for which the contribution of all the shocks on a given variable sum to 1.

[4] The object $GIRF_{Y_i}(\cdot)$ in Lanne and Nyberg's (2016) expression refers to the GIRFs à la Pesaran and Shin (1998). This definition of the GIRF refers to a non-orthogonalized shock and it can be applied both to linear and to nonlinear VAR models. Details can be found in Pesaran and Shin (1998) and Lanne and Nyberg (2016).

[5] The size of the shock matters in a nonlinear model. The use of a one standard deviation shock in all variables allows our GFEVD algorithm to return the usual Forecast Error Variance (FEV) and Forecast Error Variance Decomposition (FEVD) quantities referred to an orthogonal shock when the algorithm is applied to a standard linear VAR model.

Proxy Structural Interacted VAR models

Our reduced-form Interacted VAR model can be written as:

$$\mathbf{Y}_t = \boldsymbol{\alpha} + \sum_{j=1}^{L} \mathbf{A}_j \mathbf{Y}_{t-j} + \left[\sum_{j=1}^{L} \mathbf{c}_j unc_{t-j} \cdot conf_{t-j} \right] + \mathbf{u}_t,$$

from where the corresponding Structural IVAR model can be obtained as:

$$\mathbf{Y}_t = \boldsymbol{\alpha} + \sum_{j=1}^{L} \mathbf{A}_j \mathbf{Y}_{t-j} + \left[\sum_{j=1}^{L} \mathbf{c}_j unc_{t-j} \cdot conf_{t-j} \right] + \mathbf{B}_0^{-1} \boldsymbol{\nu}_t,$$

where $\mathbf{Y}_t$ is a vector of variables of interest, $\mathbf{A}_j$ and $\mathbf{c}_j$, $j = 1, ..., L$, are coefficient matrices and coefficient vectors, respectively, and $\boldsymbol{\nu}_t$ is a vector of economically meaningful structural shocks that are a linear combination of the reduced-form IVAR residuals, i.e., $\boldsymbol{\varepsilon}_t = \mathbf{B}_0^{-1} \boldsymbol{\nu}_t$. Suppose we are interested in partial identification and, in particular, in the impulse response of a shock $\nu_{it} \in \boldsymbol{\nu}_t$. This means that we only need to identify the i-th column of the matrix $\mathbf{B}_0^{-1}$, $\mathbf{b}_{0,i}^{-1}$. Call the other columns as $\mathbf{B}_{0,\bar{i}}^{-1}$. Consequently, we can rewrite $\boldsymbol{\varepsilon}_t = \mathbf{B}_0^{-1} \boldsymbol{\nu}_t$ as:

$$\boldsymbol{\varepsilon}_t = \mathbf{b}_{0,i}^{-1} \nu_{it} + \mathbf{B}_{0,\bar{i}}^{-1} \boldsymbol{\nu}_{\bar{i}t}$$

A Proxy Structural IVAR model allows us to identify the impact vector $\mathbf{b}_{0,i}^{-1}$ by means of an instrument m_t that satisfies the following conditions:

$$\begin{array}{cc} \mathbb{E}\left[m_t \nu_{it}\right] = \phi \neq 0 & (Relevance\ condition) \\ \mathbb{E}\left[m_t \boldsymbol{\nu}_{\bar{i}t}\right] = \mathbf{0} & (Exogeneity\ condition) \end{array}.$$

The previous conditions imply:

$$\mathbb{E}\left[m_t \boldsymbol{\varepsilon}_t\right] = \mathbf{b}_{0,i}^{-1} \phi,$$

or:

$$\begin{pmatrix} \mathbb{E}\left[m_t \varepsilon_{1t}\right] \\ \mathbb{E}\left[m_t \varepsilon_{2t}\right] \\ . \\ \mathbb{E}\left[m_t \varepsilon_{Nt}\right] \end{pmatrix} = \begin{pmatrix} \mathbf{b}_{0,i}^{-1}(1)\phi \\ \mathbf{b}_{0,i}^{-1}(2)\phi \\ . \\ \mathbf{b}_{0,i}^{-1}(N)\phi \end{pmatrix},$$

where $\mathbf{b}_{0,i}^{-1}(z)$, $z = 1, ..., N$, denotes z-th element of the vector $\mathbf{b}_{0,i}^{-1}$. Without loss of generality, assume that we are interested in the effects of the first shock, or $i = 1$. Hence with $\mathbb{E}[m_t \boldsymbol{\varepsilon}_t]$ in hand we can recover the normalized impact vector as:

$$\begin{pmatrix} 1 \\ \frac{\mathbb{E}[m_t \varepsilon_{2t}]}{\mathbb{E}[m_t \varepsilon_{1t}]} \\ . \\ \frac{\mathbb{E}[m_t \varepsilon_{Nt}]}{\mathbb{E}[m_t \varepsilon_{1t}]} \end{pmatrix} = \begin{pmatrix} 1 \\ \frac{\mathbf{b}_{0,1}^{-1}(2)}{\mathbf{b}_{0,1}^{-1}(1)} \\ . \\ \frac{\mathbf{b}_{0,1}^{-1}(N)}{\mathbf{b}_{0,1}^{-1}(1)} \end{pmatrix},$$

which corresponds to the impact vector for an unitary shock, $\left[1; \mathbf{b}_{0,1}^{-1}(\bar{1})/\mathbf{b}_{0,1}^{-1}(1)\right]$. An estimate of $\mathbf{b}_{0,1}^{-1}(\bar{1})/\mathbf{b}_{0,1}^{-1}(1)$ can be obtained from the two stage least square regression of $\boldsymbol{\varepsilon}_{\bar{1}t}$ on ε_{1t} using the instrument m_t. The first stage regression:

$$\varepsilon_{1t} = \beta m_t + \xi_t$$

yields the fitted values $\hat{\varepsilon}_{1t}$, which are then used in the second stage regression to recover the true normalized impact vector:

$$\begin{aligned} \boldsymbol{\varepsilon}_{\bar{1}t} &= \boldsymbol{\gamma}\hat{\varepsilon}_{it} + \boldsymbol{\varsigma}_t. \\ &= \frac{\mathbf{b}_{0,1}^{-1}(\bar{1})}{\mathbf{b}_{0,1}^{-1}(1)}\hat{\varepsilon}_{it} + \boldsymbol{\varsigma}_t, \end{aligned}$$

where the recoverability of $\mathbf{b}_{0,1}^{-1}(\bar{1})/\mathbf{b}_{0,1}^{-1}(1)$ depends on the fact that $\mathbb{E}[m_t \boldsymbol{\varepsilon}_t] = \mathbf{b}_{0,1}^{-1}\phi$.[6]

The (absolute) impact vector $\mathbf{b}_{0,1}^{-1}$ can then be derived from the estimated reduced form variance-covariance matrix, $\Sigma = \mathbb{E}[\boldsymbol{\varepsilon}_t \boldsymbol{\varepsilon}_t']$, as explained, e.g., in Gertler and Karadi (2015).[7] At this point we can compute the impulse response function to a one standard deviation shock in date t, $\delta_t = 1$, to

[6] Indeed, we have: $\gamma = \frac{\mathbb{E}\left[\boldsymbol{\varepsilon}_{\bar{1}t}\hat{\varepsilon}_{it}\right]}{\mathbb{E}\left[\hat{\varepsilon}_{it}^2\right]} = \frac{\mathbb{E}\left[\boldsymbol{\varepsilon}_{\bar{1}t}\beta m_t\right]}{\mathbb{E}\left[\beta^2 m_t^2\right]} = \frac{\beta\mathbb{E}\left[\boldsymbol{\varepsilon}_{\bar{1}t} m_t\right]}{\beta^2\mathbb{E}\left[m_t^2\right]} = \frac{\frac{\mathbb{E}[\varepsilon_{1t} m_t]}{\mathbb{E}\left[m_t^2\right]}\mathbb{E}\left[\boldsymbol{\varepsilon}_{\bar{1}t} m_t\right]}{\left(\frac{\mathbb{E}[\varepsilon_{1t} m_t]}{\mathbb{E}\left[m_t^2\right]}\right)^2 \cdot \mathbb{E}\left[m_t^2\right]} = \frac{\mathbb{E}\left[\boldsymbol{\varepsilon}_{\bar{1}t} m_t\right]}{\mathbb{E}[\varepsilon_{1t} m_t]} = \frac{\phi \mathbf{b}_{0,1}^{-1}(\bar{1})}{\phi \mathbf{b}_{0,1}^{-1}(1)}$.

[7] Specifically, to recover the absoulte impact vector we follow Piffer's notes on the identification of VARs using external instruments available at https://sites.google.com/site/michelepiffereconomics/ .

ν_{1t}, according to the usual Generalized IRF à la Koop, Pesaran, and Potter (1996):

$$\begin{aligned} GIRF_{Y,t}(h,1,\boldsymbol{\varpi}_{t-1}) &= \mathbb{E}\left[\mathbf{Y}_{t+h} \mid \delta_t = 1, \boldsymbol{\varpi}_{t-1}\right] - \mathbb{E}\left[\mathbf{Y}_{t+h} \mid \boldsymbol{\varpi}_{t-1}\right], \text{ for } h = 0, 1, ..., H \\ &= \begin{cases} \mathbf{b}_{0,1}^{-1} & \text{, for } h = 0 \\ \mathbb{E}[\mathbf{Y}_{t+h} \,|\delta_t = 1, \boldsymbol{\varpi}_{t-1}] - \mathbb{E}[\mathbf{Y}_{t+h} \mid \boldsymbol{\varpi}_{t-1}] & \text{, for } h = 1, ..., H \end{cases}, \end{aligned}$$

where $\boldsymbol{\varpi}_{t-1}$ denotes the initial condition, or $\{\mathbf{Y}_{t-1}, ..., \mathbf{Y}_{t-L}\}$. In computing the GIRF we follow the same algorithm outlined earlier.

Supplementary results

Figure A1 plots the time series that enter our baseline IVAR.

Figure A2 plots the daily VSTOXX index, our proxy for euro area financial uncertainty, against its monthly average.

Figure A3 in its upper panel plots the consumer confidence indicator released by the european Commission in April – a leading indicator of future economic activity –, which signaled a confidence level approaching the number reached during the 2008-2009 financial crisis. The bottom panel of Figure A3 plots the monthly VSTOXX, our baseline measure of financial uncertainty, which in March 2020 reached levels comparable to the global financial crisis.

Figure A4 plots all the uncertainty indicators we use in our analysis, as described in the robustness checks Section of the paper.

Figure A5 plots all the indices of survey-based confidence we use in our analysis, as described in the robustness checks Section of the paper.

Figure A6 plots the pessimistic-times state under the alternative interpretation of pessimism based on "mood swings", i.e., sudden negative changes in the consumer confidence series. We classify an initial month to the pessimistic-times state whenever the cumulative change in the last six months of the Consumer Confidence Index is in its bottom 20%.[8] In this way, pessimistic times only include phases of negative mood swings.

Figure A7 documents that our main results are not driven by the baseline definition of our pessimistic-times state, based on the bottom quintile of the historical distribution of consumer confidence. We alternatively use the bottom decile, the bottom tertile, and the median as the relevant thresholds.

[8] This threshold corresponds to a cumulative change of -2.5.

Figure A8 shows how the impulse response of industrial production and inflation change at the different quintiles of the historical distribution of confidence (for the sake of clarity we only show the impulse response at five steps ahead, which is the trough of the impulse response of the linear model). The Figure shows that the impact of uncertainty shocks gradually increases as the economy's outlook (in the initial condition) dampens.

References

Andreasen, M. M., J. Fernández-Villaverde, and J. F. Rubio-Ramírez (2017): "The pruned state-space system for non-linear DSGE models: Theory and empirical applications," *The Review of Economic Studies*, 85(1), 1–49.

Caggiano, G., E. Castelnuovo, and G. Pellegrino (2017): "Estimating the Real Effects of Uncertainty Shocks at the Zero Lower Bound," *European Economic Review*, 100, 257–272.

Christiano, L. J., M. Eichenbaum, and C. Evans (1999): "Monetary Policy Shocks: What Have We Learned and to What End?," In: J.B. Taylor and M. Woodford (eds.): Handbook of Macroeconomics, Elsevier Science, 65–148.

Gertler, M., and P. Karadi (2015): "Monetary Policy Surprises, Credit Costs, and Economic Activity," *American Economic Journal: Macroeconomics*, 7(1), 44–76.

Kilian, L., and R. Vigfusson (2011): "Are the Responses of the U.S. Economy Asymmetric in Energy Price Increases and Decreases?," *Quantitative Economics*, 2, 419–453.

Koop, G., M. Pesaran, and S. Potter (1996): "Impulse response analysis in nonlinear multivariate models," *Journal of Econometrics*, 74(1), 119–147.

Lanne, M., and H. Nyberg (2016): "Generalised Forecast Error Variance Decomposition for Linear and Nonlinear Multivariate Models," *Oxford Bulletin of Economics and Statistics*, 78, 595–603.

Pellegrino, G. (2017): "Uncertainty and Monetary Policy in the US: A Journey into Non-Linear Territory," Melbourne Institute Working Paper No. 6/17.

Pesaran, H. M., and Y. Shin (1998): "Generalized Impulse Response Analysis in Linear Multivariate Models," *Economics Letters*, 58, 17–29.

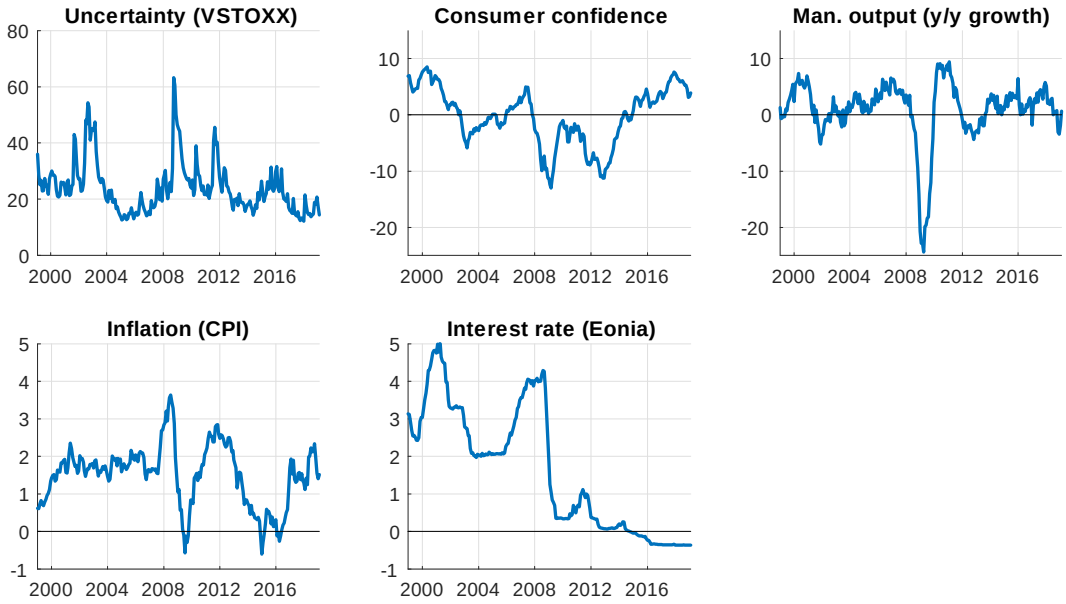

Figure A1: **Time series modeled in our baseline IVAR model.** *Note*: the series and their sources are given in Section 2 of the main paper. The sample period modeled is 1999m1-2020m1.

Figure A2: **VSTOXX index since January 2020.** Black solid line: daily index. Black dashed line: monthly average.

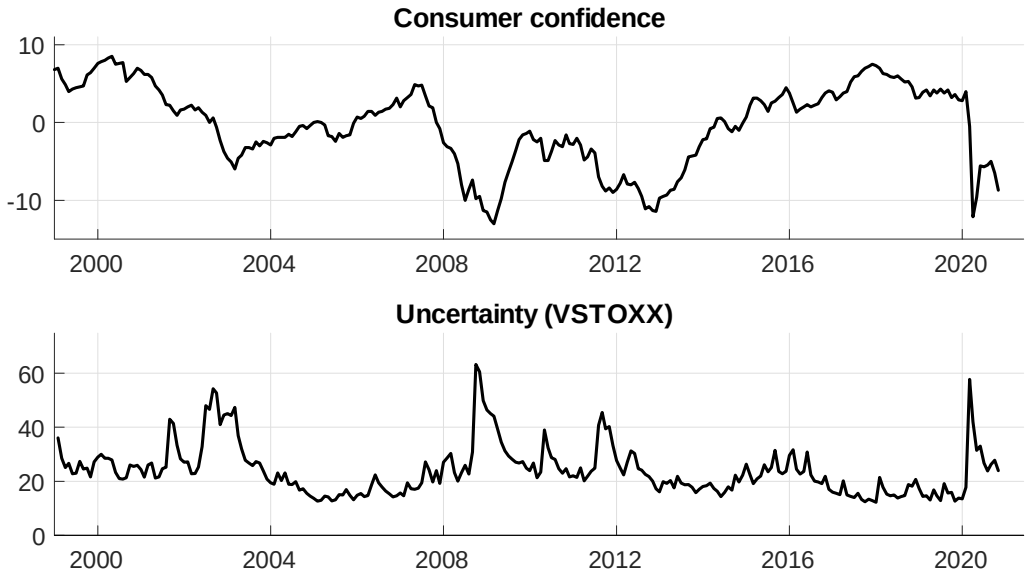

Figure A3: **Consumer Confidence and Uncertainty.** Top panel: European Commission Consumer Confidence Index**.** Bottom panel: VSTOXX. *Note*: 1999m1-2020m10.

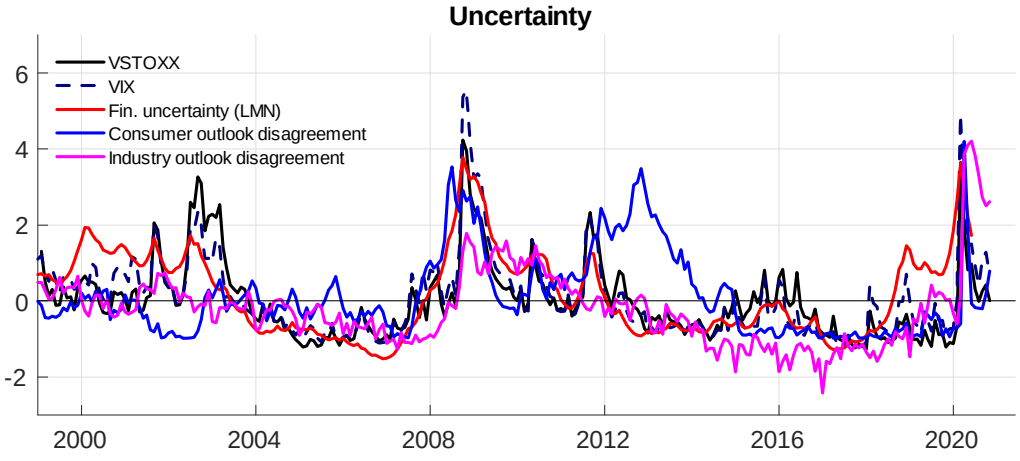

Figure A4: **Uncertainty indicators**. *Note*: 1999m1-2020m11. Each series is standardized to have 0 mean and unit variance to make the series comparable.

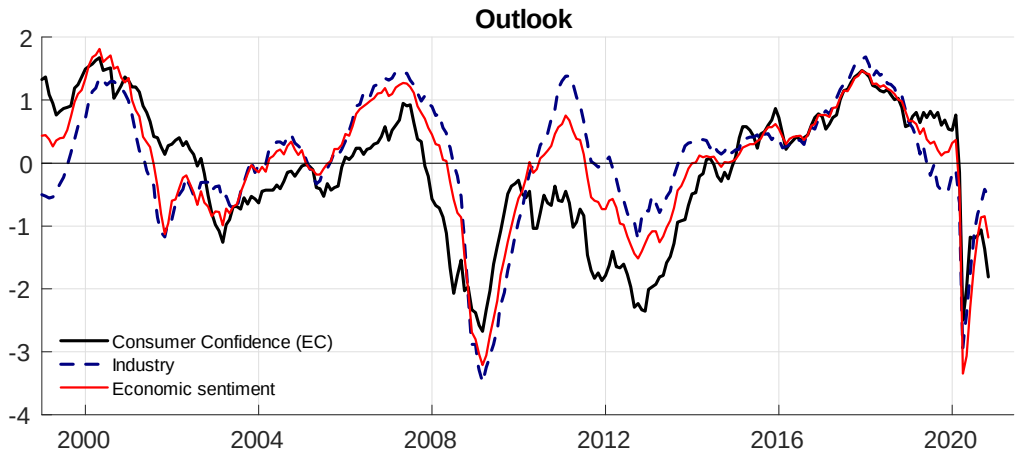

Figure A5: **Survey-derived measures of confidence**. *Note*: 1999m1-2020m10. Each series is standardized to have 0 mean and unit variance to make the series comparable.

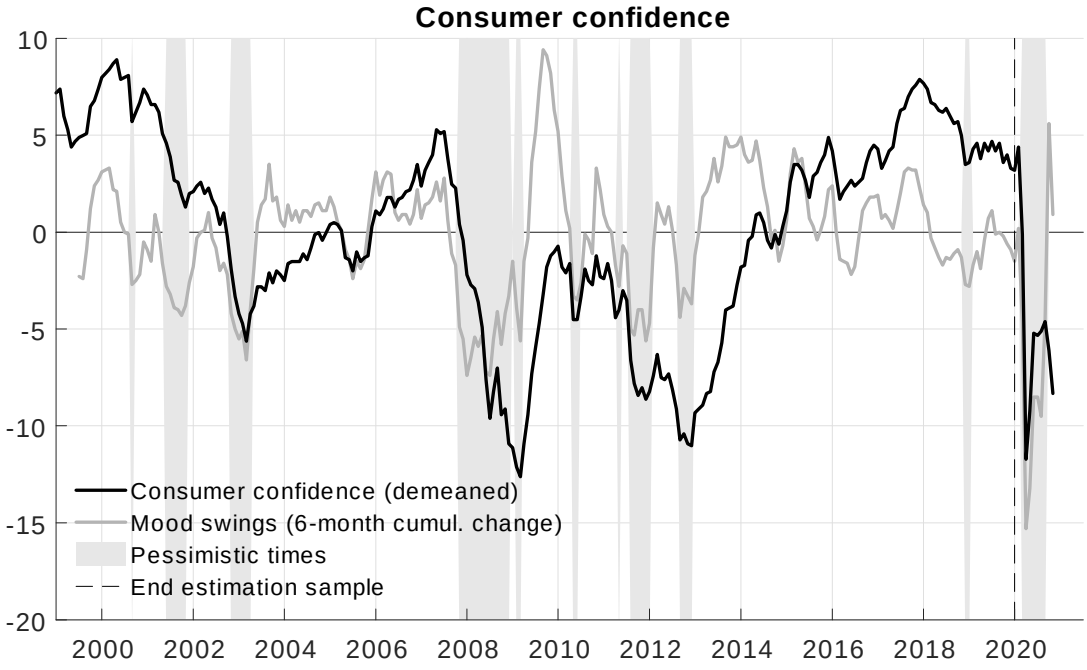

Figure A6: **Alternative definition of pessimistic times based on "mood swings"**. Black solid line: EC Consumer Confidence Index. Gray line: Cumulative change in the last six months of the Consumer Confidence Index. Gray vertical bars: Initial quarters with the bottom 20% cumulative change in the last six months of the confidence series defining the pessimistic times state. Vertical black dashed line: Denotes the end of the estimation sample.

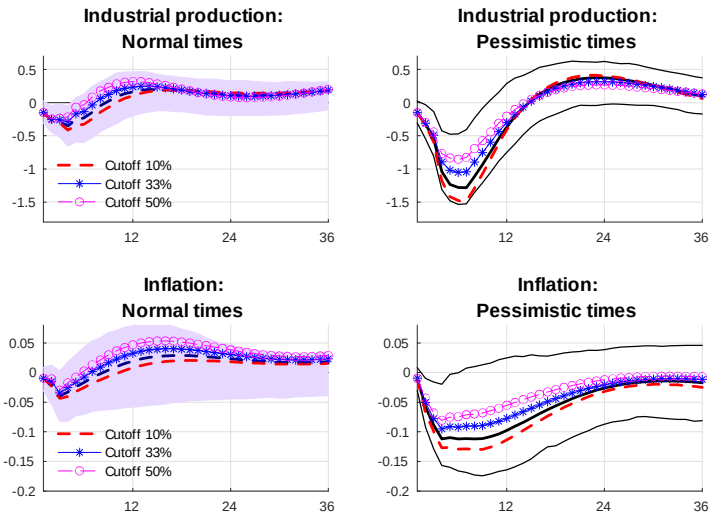

Figure A7: **Further robustness to alternative IVAR specifications.** Top panels: Industrial Production GIRFs. Bottom Panels: Inflation GIRFs. Left-hand-side panels: Blue dashed lines and light blue areas represent the point estimates and 90% bootstrapped confidence bands for the baseline industrial production GIRFs conditional on normal times. Right-hand-side panels: Black solid lines represent the point estimates (bold lines) and 90% bootstrapped confidence bands for the baseline industrial production GIRFs conditional on pessimistic times. For the other lines refer to the legend and the main text. Monthly data.

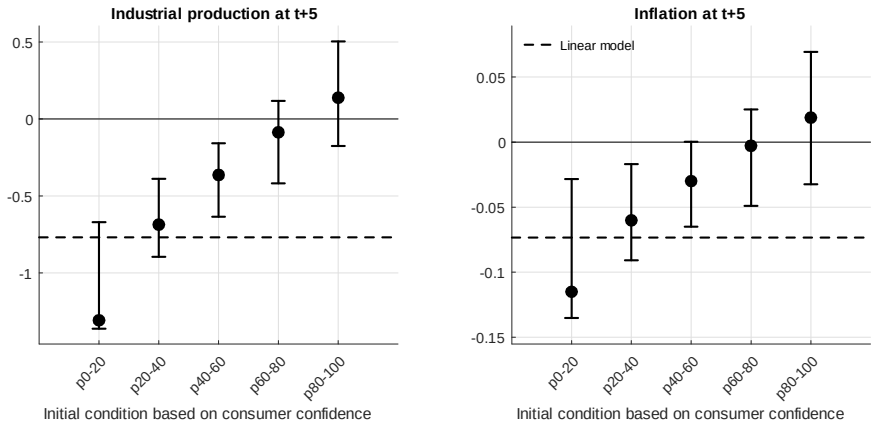

Figure A8: **Impulse responses at different quintiles of the confidence distribution.** Left-hand-side panel: Industrial production. Right-hand-side panel: Inflation. Black dots: Point estimates of the impulse responses at five steps ahead for the alternative sets of initial conditions referring to each quantile of the confidence distribution. Black bars: 68% bootstrapped confidence bands. Dashed black lines: Point estimates of the impulse responses for the nested linear VAR model.